COVER SHEET

Conceptual Fracture Parameters for Articular Cartilage

K. Stok and A. Oloyede

School of Mechanical, Manufacturing and Medical Engineering
Queensland University of Technology, Gardens Point
2 George Street, GPO Box 2434, BRISBANE
QUEENSLAND, AUSTRALIA.

Correspondence and reprints to: A/Professor A. Oloyede, School of Mechanical, Manufacturing and Medical Engineering, Queensland University of Technology, Gardens Point, GPO Box 2434, Brisbane, Queensland, Australia.
email: k.oloyede@qut.edu.au

Abstract

Background

Superficial cracks can occur in articular cartilage due to trauma or wear and tear. Our understanding of the behaviour of such cracks in a loaded matrix is limited. A notable study investigated the growth of cracks induced in the bottom layer of the matrix. This paper extends existing studies, characterizing the propagation of superficial cracks and matrix resistance under tension at varying rates of loading.

Methods

Cartilage strips with artificially induced superficial cracks were subjected to tensile loading at different loading velocities using a miniature tensile testing device. Load-displacement data, video and still images were recorded for analysis.

Findings

The propagation of superficial cracks in articular cartilage does not follow the classical crack tip advance that is characteristic of most engineering materials. Instead, the crack tip exhibited a negligible movement while the side edges of the crack rotated about it, accompanied by matrix stretching and an upward pull (necking) of the bottom layer of the sample. As loading progresses, the crack edges stretch and rotate to assume a position parallel to the articular

surface, followed by the final fracture of the matrix at a point just below the crack tip. Using the recorded mechanical data and images, an analogous poroelastic fracture toughness, Kp_{IC} = 1.83 MPa.$\sqrt{\text{mm}}$ (SD 0.8) is introduced.

Interpretation

It is extremely difficult for a superficial crack to propagate through articular cartilage. This may be because of the energy dissipation from the crack due to the movement and exudation of water, and large stretching of the matrix.

Keywords : soft tissue fracture, superficial zone cracks, crack propagation in articular cartilage, poroelastic fracture toughness, mechanical damage

1. Introduction

Several authors have reported that micro-mechanical damage to the articular surface due to trauma and overloading could initiate the osteoarthritic process in articular cartilage, and overall joint malfunction (McCormack and Mansour 1998, Frost 1999). A fundamental biomechanical question addressed in this present work is that of how to quantify the resistance of the loaded cartilage matrix to the growth of a microcrack initiated in its superficial layer. Fracture mechanics theory stipulates that it is either the critical value of the stress intensity factor or energy release rate, i.e. fracture toughness, which governs the response of a given material to crack propagation. Also it is well established that certain geometrical relationships must exist between the crack size, length, width and thickness of a specimen before it can be used to satisfactorily determine the fracture toughness of a material. The literature on cartilage fracture toughness (Chin-Purcell and Lewis 1996) is unclear as to what specimen geometrical constraints must hold before there can be confidence in any value of cartilage fracture toughness. Fracture toughness is a material property that has been evaluated for several elastic and elastic-plastic materials in the literature. However, the poro-hyperelastic nature of articular cartilage in which water plays a significant role in load-carriage, suggests the need for a critical appraisal of classical methods in establishing the fracture parameters for this tissue. Consequently, in this study we have devised a methodology for studying the fracture propagation characteristics of the cartilage matrix and proposed a quantitative evaluation of its ability to resist crack growth.

1.1 Structure and Function

Articular cartilage is the tissue that covers the ends of bones in articulating joints of humans and animals. Its role is to provide a well-lubricated, low friction, bearing surface for smooth, resistance-free, joint movement (Radin et al. 1973). This aids in the distribution and transmission of applied loads to the underlying bone structure (Radin et al 1973, Kempson et al. 1971).

Glenister (1976) proposed that articular cartilage could be divided into four macroscopic layers. The superficial zone or articular surface is the uppermost layer. This layer is known to be more resistant to wear (Lipshitz et al. 1976) and stronger in tension (Clarke 1971) than the underlying layers, yet it is also the first layer to show cracking as a result of overstressing (Meachim and Roy 1969). Below the articular surface lie the middle, deep and calcified zones. Since the properties of the tissue derive from the interaction between these structurally dissimilar layers, we will investigate crack propagation through the entire matrix.

The stresses experienced by the articular cartilage during everyday activities are a combination of dynamic and inertial loads. Morrison (Morrison 1970, Morrison 1968) found that during the walking cycle the knee experiences forces of 2.06 to 4 times body weight. In addition, a compression of 0.42 to 3.40 times body weight is experienced in the tibio-femoral joint during maximum isomeric contraction of the knee joint (Finlay and Repo 1979).

In order to alleviate the effect of these high stresses in the subchondral bone, cartilage undergoes a complex interaction between its fluid and solid components resulting in controlled deformation in each of its disparate layers (Kempson et al. 1971, Meachim 1980), influencing the patterns of crack propagation.

In addition, it has been shown (Oloyede et al. 1992, Radin et al. 1970) that the compressive response of the cartilage matrix is strongly dependent on strain-rate (for example, $\dot{\varepsilon} = 5\text{x}10^{-5}\text{s}^{-1}$ to 10^{3}s^{-1}). At progressively higher strain-rates, the matrix stiffness increases to a limiting value at impact (Oloyede et al. 1992). The stiffening at high loading rates can be expected to render the matrix more susceptible to fracture in a manner that can be considered relevant to the effects of trauma and osteoarthritis (Kempson et al. 1971), while the fluid-controlled poroelastic deformation would affect crack behaviour under low rates of loading. The pertinent questions in this study are therefore that of (i) how fracture resistance is manifested in articular cartilage, (ii) whether or not there is a unique value which is truly geometry and rate

independent, i.e. fracture toughness, and (iii) whether or not such a parameter can be realistically quantified.

1.2 Pertinent Fracture Mechanics

1.2.1 The Tensile Opening Mode

Although crack growth in cartilage involves a significant amount of stretching, in this study we will examine the opening mode of fracture (Ewalds and Wanhill 1991) subject to the expression:

$$K_I = \sigma\sqrt{(\pi.a)}.f\left(\frac{a}{W}\right) \quad (1)$$

Or

$$K_I = \frac{P}{BW^{\frac{1}{2}}}.f\left(\frac{a}{W}\right) \quad (2)$$

where K_I is Mode I stress intensity factor, σ = applied stress, a = crack length, B = specimen width, W = specimen thickness, P = force (load), *f(a/W)* is a geometrical factor allowing for specimen and crack geometry (ASTM 1990), and π is a constant.

The parameters in equations 1 and 2 will be examined for cartilage fracture mechanism would require quantification for articular cartilage in the light of its peculiar elastic behaviour and concomitant unconventional fracture propagation pattern (see figure 1 and (Stok and Oloyede 2003)). Of these parameters the geometrical correction factor *f(a/W)* poses a real problem, due to the fact that the intrinsic thickness of articular cartilage makes it practically impossible to define a plane strain condition in the manner reported in the standards for conventional engineering materials.

1.3 Fracture Mechanics and Articular Cartilage Deformation

1.3.1 Mechanism of failure

The mechanism of crack propagation in articular cartilage was reported earlier (Stok and Oloyede 2003). This demonstrated a large stretch accompanied crack growth, with

collagen fibres contributing by pulling up the bottom layers of the matrix creating necking and ultimately failure within the midzone matrix.

1.3.2 Published fracture toughness of articular cartilage

In the work referred to earlier, Chin-Purcell and Lewis (1996) quantified the fracture toughness of cartilage, using a modified single-edge notch test to measure a J-integral-based toughness, and a trouser tear test to measure tearing toughness as defined by Rivlin and Thomas (1953). In agreement with Purslow (1983), they obtained J-toughness values of between 0.14 and 1.2kN/m, which were about 1.7 times greater than those from trouser tear fracture toughness values of 0.24 to 0.8kN/m; using he J-integral to determine the fracture toughness and assuming that the rate of viscous and plastic dissipation in the tissue was negligible. Chin-Purcell and Lewis (1996) also assumed small strain in their derivation of the J-integral, and showed that although there will be large strain deformation at the notch root, if it is fully contained in this region it will not affect the J-integral derivation.

In the study of Chin-Purcell and Lewis (1996) the fracture toughness of the tissue was obtained from samples whose superficial layers had been removed, so that the notch was initiated in the deep zone and propagated toward the surface. It is our opinion that a more beneficial study is one in which the initiated crack is initiated in the superficial layer and propagated through the general matrix, since it is known that initial damage, i.e. fissures or microcracks, are usually initiated in the articular surface (Meachim 1972). Furthermore, none of the recorded studies of cartilage fracture established the influence of factors such as specimen thickness, size of initial crack, or loading rate. Therefore, in the present analysis we will maintain the structural integrity of the matrix initiated a crack if known micro-depth in the superficial layer and subject it to known tensile loads at known velocities, to mimic the more probable situation in vivo.

2. Materials and Methods

2.1 Specimen Preparation

Patellae of freshly slain bovine animals (3-4 years) were obtained from the local abattoir and stored at –20^{o}C. Just before the commencement of testing, the patellae were thawed and the surrounding soft tissue was removed. A double-bladed cutter was used to slice parallel sections of cartilage while it was still attached to the bone. All specimens were cut along an apex-base orientation. The cartilage was shaved off the bone in the customary manner of Broom, for example in (Broom 1984). Specimens were stored in individually labelled vials containing physiological saline (0.15M) until just prior to mounting on the mini tensile testing equipment.

The specimens tested were cut to widths, B, of between 0.5 and 2.5mm, shown in figure 2, in accordance with American Society for Testing and Materials (ASTM) standards regarding a $^{B}/_{W}$ ratio of ~0.5 (ASTM 1990). This was possible by cutting to appropriate blade separation settings of the double-bladed cutter. Overall 363 specimens harvested from 32 joint samples were tested.

2.2 Repeatability Tests

The mini tensile tester was verified to ensure that the load cell and displacement transducer outputs were accurate. These results can be found in (Stok and Oloyede 2003). It was established that measurements acquired by the mini tensile tester are equivalent to those from a commercially available machine such as the Hounsfield.

2.3 Tensile Tests

A miniature tensile testing apparatus was purpose-built for testing articular cartilage in tension at varying strain-rates. The apparatus is described in detail in (Stok and Oloyede 2003).

The specimen was placed into the tensile tester grips with fresh emery paper, and tissue glue, LOCTITE 454 (Loctite, Australia PTY Ltd New South Wales Australia), between the paper and the specimen. One hundred specimens were tested at loading rates,

$\dot{\varepsilon} = 0.0016\text{s}^{-1}$, 0.0032s^{-1}, and 0.0048s^{-1}, thereby testing a total of 300 specimens. Each specimen was tested under tension at a nominated loading rate up to a strain of 10%, unloaded and allowed to recover completely to its initial unloaded length, before laceration and further loading. These preloading tests were conducted in order to determine the stiffness of the various specimens before initiating cracks in them, so that they could be categorised into groups of similar stiffness for subsequent analysis. The stress-strain data were stored using LABVIEW.

2.4 Fracture Tests

After obtaining the intrinsic mechanical properties of a given specimen, and after full recovery, a custom-built surface lacerator, which could be preset to an incision depth, was used to lacerate the articular surface to a designated depth to simulate a crack of known dimensions. Using this methodology, initial pre-loading cracks of a_i = 0, 25, 50, 75, or 100μm were inflicted wholly within the articular surface, which is 150-200μm deep (Broom and Marra 1985).

Each specimen was tested until failure at the same loading rates that were used for the initial test mentioned above depending on the specimen set. Twenty tests were carried out for each crack length, at each of the three loading rates, $\dot{\varepsilon} = 0.0016\text{s}^{-1}$, $\dot{\varepsilon} = 0.0032\text{s}^{-1}$, and $\dot{\varepsilon} = 0.0048\text{s}^{-1}$ respectively, so that a total of 300 specimens were tested. The stress-strain data were logged and stored using LABVIEW.

2.5 Direction and Site Dependence

Akizuki (Akizuki et al. 1986) previously observed that the mechanical properties of the tissue could vary with site, i.e. location on the joint. Consequently, to establish the integrity of these results with respect to the known characteristics of articular cartilage, it is necessary to investigate the dependency of samples on their location within the joint. All specimens were therefore categorised according to their location on the patellar surface.

Secondly, all specimens were pinpricked three times along their length at the conclusion of mechanical testing to verify split-line orientation so as to determine whether or not there is a dependence of fracture properties on split-line orientation in a specimen. All specimens were cut from the bone in a caudo-cranial (apex-base, a-b) lengthwise direction, with the artificial crack cut in the medio-lateral (m-l) direction. When the specimens were pinpricked to determine the split-line direction, the split-lines were categorised as lying either m-l or a-b. (Split-lines lying at 'in-between' angles were categorised according to their predominant direction.) Since three splits were made in one specimen, a predominant direction could easily be identified. So it can be said that each tensile test was conducted either along the split-line (a-b), or across the split-line (m-l).

2.6 Digital Analysis

Another 63 specimens were tested at a higher magnification of 20 x to ensure visual accuracy for digital analysis. Following the methodology outlined earlier, three specimens were tested at each speed for crack lengths, a_i of 0, 25, 50, 75, 100, 150 and 200μm, that is *3 specimens x 3 loading rates x 7 crack lengths*. The data captured was converted to digital video (i.e. .avi files). It was then digitally analysed using Video Expert II (Motion Anaylsis Corp. Santa Rosa, CA, USA) to investigate crack growth and crack growth rates through the thickness of each specimen.

3. Results

3.1 Stress-Strain Curves for Articular Cartilage Mode I Fracture

Figure 3 shows the relationship between typical stress-strain curves, rate of loading ($\dot{\varepsilon}$ = 0.0016, 0.0032 and 0.0048 s^{-1}), and initial crack length, a_i = 25 and 100μm. The specimens with crack lengths of 25μm typically displayed a higher maximum stress than those with 100 μm cracks, at all rates of loading, figure 3(a-c). It can also be seen that the tangent moduli appear to be of a similar value for the three rates of loading, and the 25 and 100μm levels, figure 3(d, e).

Tables 1 and 2 present the data on the dependence of the average mechanical properties of the samples on site within the joint. It can be concluded that the mean values of the maximum load, stress, and strain energy per unit volume for the medial and lateral aspects were similar. There is a slight difference in the mean tangent moduli of the medial and lateral samples when the modulus was taken at the 20% strain level. However, this is not reflected in compliance measurements.

A separation of the compliance data with respect to the rate of loading was also considered using a one-way analysis of variance (ANOVA). It can be seen from the large p-values (Table 2) that the compliance were similar for both the lateral and medial samples at all strain-rates, and also that the material is more compliant at small strains.

This analysis was repeated for initial crack lengths. Again it was found that the mean compliance at different initial crack lengths can be considered practically equal for both the lateral and medial aspects (Table 3). Although for the lateral aspect at the 20% strain level, there was some evidence for an increasing compliance with crack length. The strain-rates in this study were chosen according to ASTM standards for fracture testing, and it should be mentioned that they only cover a narrow range of the physiologically relevant loading rates, and strain-rate effects may occur at higher strain-rates.

3.2 Examination of Direction Dependence of Material Properties

A similar examination was conducted to ascertain whether or not there were any differences between the properties of specimens tested along or across the split line direction. A comparison of the failure stress for the two different orientations presented on Table 4 shows that there is a significant difference (p-value = 0.002%). Similarly, a comparison of tangent moduli at the 2.5% and 20% strain levels (shown in Table 4), demonstrates that the tangent modulus at 2.5% strain is slightly higher in the m-l direction. However at higher strains, there is a slightly more

strain-limiting behaviour for specimens lying along the split-line direction (a-b). This is also reflected in the compliance values and is confirmed in the stress-strain curves (fig. 3).

The data was separated with respect to strain-rate, and an ANOVA was conducted. It was found that the compliance was similar at all strain-rates for both the medio-lateral and apex-base orientations at the 2.5% and 20% strain levels (Table 5).

This analysis was repeated for each initial crack length. It was found that compliance was similar at all crack lengths, for both the m-l and a-b orientations at the 2.5% strain levels (Table 6). There is some evidence, albeit inconclusive, to suggest that compliance increases with crack length at the 20% strain level, for both the m-l and a-b orientations. These results compare well with the typical stress-strain curves shown in figure 3.

3.3 Comparison of rate of crack growth at different strain-rates

For the majority of specimen stress-strain curves, there was a phase of rapid crack propagation, which suddenly stopped and was then followed by a brief period of stable propagation, before final catastrophic failure. The load carried by the articular cartilage tissue in this period dropped dramatically as the crack rapidly grew through the matrix. This change in stress ($\Delta\sigma$) was measured and analysed to establish whether or not it is related to the rate of loading, see figure 3. It should be noted that this region in which $\Delta\sigma$ is measured is the unloading one, indicating crack growth. The load carried by the articular cartilage tissue in this period of rapid propagation dropped dramatically as the crack travelled through the matrix. It can be seen in figure 4 that $\Delta\sigma$ does not vary significantly for the different loading rates. We therefore propose that it is the structural variations between the different zones of the tissue, rather than the speed of loading, that primarily determine the characteristics of fracture in articular cartilage.

3.4 The Poroelastic "Fracture Toughness" of Articular Cartilage

It has been shown that fracture of articular cartilage can be characterised by curves such as those shown in figure 5, where it can also be seen that the propagation of the initial crack commences at point A and is then followed by rapid propagation (unloading) through the general matrix

(section AB), and then a period of energy accumulation and no growth (BC) before final fracture (CD). This interpretation is consistent with the general principle of crack growth in classical fracture mechanics where unloading is well recognised to represent crack propagation. We have also identified portions of the curve in this manner because it is apparent from our experiments that the rest of the matrix offers significantly little or no resistance to fracture propagation once the articular surface had been completely fractured; this is represented by the very low slope of the region BC in figure 5 which characterises the resistance of the material to the applied load and deformation. In this respect a high slope of the region BC would have conveyed the ability of the matrix to continue to offer any substantial resistance to the propagating crack after the crack growth that would have occurred in the period represented by the region AB of the curve. Consequently, we have correlated the stress-strain data and the crack growth pictures to determine these critical points. To this end the maximum energy developed before unstable crack growth was evaluated as the area under the curve OA of figure 5. This is the critical strain energy per unit volume which would cause catastrophic failure of the tissue, when a crack is initiated and confined within its superficial zone.

Our experimental results demonstrate that the initiated surface crack is propagated through transverse opening, accompanied by a radial upward pulling of the deep matrix which develops as a wavefront-type growth (Stok and Oloyede 2003). Our analysis revealed that transverse crack opening can be defined by the combined change in length or stretch, *dc*, which is made up of crack dimensions *a* and *b*, as shown in figure 1. Furthermore, we have established that the length *dc*, or transverse extension is equivalent to the rate of necking, *dh*. These results show that the crack stretch Δc can be used as a measure of crack growth because it is directly related to the radial or vertical dimension, *dh*, of wavefront crack growth shown in figure 1.

The above findings have been used for suggesting a new fracture parameter, namely the poroelastic fracture characterisation parameter Kp_{Ic}. The Kp_{Ic} is evaluated at the first instance of

precipitous load. The critical opening stress, σ_{op} was identified for all curves displaying typical stress-strain curves as that stress at the first instance of precipitous load. The corresponding crack geometry parameter during the typical stretch or lateral opening, c_{ps} of the crack at this point was evaluated by matching stress-strain curve data and visual inspection. Relative to the above and borrowing from the well-known fracture mechanics fracture toughness expression, the experimental data was fitted to obtain Kp_{Ic},

$$Kp_{Ic} = \sigma_{op}\sqrt{\pi.c_{ps}} \tag{3}$$

3.5 Test for the validity of Kp_{Ic}

For the calculated values of Kp_{Ic}, the variation with rate of loading, $\dot{\varepsilon}$, or initial crack length, a_i, must be considered. Therefore, a one-way analysis of variance, ANOVA was used to test if the mean Kp_{Ic} values for $\dot{\varepsilon}$ = 0.0016, 0.0032 and 0.0048s^{-1} were equal. This test does not consider the effect of initial crack length. A large p-value (0.761) demonstrates that the three means can be considered practically equal, and there is no variation in poroelastic fracture parameter, Kp_{Ic} with rate of loading.

A second ANOVA was performed to determine the effect of initial crack length. This test does not consider the effect of rate of loading. A large P-value (0.665) demonstrates that there is no significant variation in the mean values, and therefore no variation in the poroelastic fracture parameter, Kp_{Ic} with initial crack length.

Finally a two-way ANOVA was conducted to determine if there is any interaction between strain-rate and initial crack length, and the determination of poroelastic fracture toughness, Kp_{Ic}. The results support the previous findings that Kp_{Ic} is not dependent on either the rate of loading or initial crack length.

Figure 6 shows that there is an appreciable scatter in the fracture toughness parameter plotted against the initial crack length relative to the rate of loading. We note that this degree of scatter, while appreciable is not significant when compared to the variation that usually accompanies

the biomechanical data obtained from various articular cartilage samples, even when tested at the same strain rate. Consequently, we argue that the effects of loading velocity and initial crack length on this novel poroelastic fracture parameter, Kp_{Ic}, are minimal. The data presented in figure 6 was therefore used to determine an average Kp_{Ic} = 1.83 MPa.$\sqrt{\text{mm}}$, (SD = 0.8) over all the strain rates applied and the initial crack sizes shown on the figure.

3.6 Comparison of Poroelastic Fracture parameter Kp_{Ic} with Previous Published Values

Firstly, in contrast to published solutions for *f(a/W)*, the variation of Kp_{Ic} using critical crack stretch, c_{ps} is quite small, figure 7. These results seem to suggest that the geometrical factors given in the literature for fracture testing of conventional materials are for specimens of much larger geometrical dimensions, especially relative to thickness, than those associated with articular cartilage, and may not be practical for the samples in our experiments. Furthermore, the thickness-width ratio of the articular cartilage matrix, where the matrix thickness is naturally between 1 and 4 mm, and $^{B}/_{W}$ of between 0.45 and 3.9, seem to suggest that the fracture of articular cartilage falls within plane stress analysis in conventional fracture mechanics.

Chin-Purcell and Lewis (1996) quoted values of fracture toughness, J = 0.14-1.2kN/m, and values of predicted Young's modulus, E = 4.95-8.93MPa. In this work, for undamaged specimens at strain-rates of 0.0016, 0.0032 and 0.0048s^{-1}, the tangent moduli at the 2.5% and 20% strain levels were evaluated and presented in table 7.

The moduli at the 2.5% strain level were approximately the same for each strain-rate, with an average of 4.55MPa (SD 1.75). Similarly the average of the moduli taken at the 20% level was practically 6.30MPa (SD 2.37) for the three strain-rates.

Using these values of tangent moduli, the critical poroelastic strain energy release rate, Gp_{Ic} could be calculated from equation 4, yielding the results shown in table 8.

$$Gp_{Ic} = \frac{Kp_{Ic}^{\,2}}{E} \qquad (4)$$

where Kp_{Ic} = 1.83 (0.8) MPa.$\sqrt{\text{mm}}$,

$E_{2.5\%}$ = 4.55 (1.75) MPa,

and $E_{20\%}$ = 6.30 (2.37) MPa.

4. Discussion

A conceptual basis for adapting classical fracture mechanics to the study of crack propagation in articular cartilage has been presented leading to the determination of fracture characterization parameter for the tissue based on a rigorous experimental study of the mechanism of crack propagation through the cartilage matrix (Stok and Oloyede 2003). Micro-deep artificial cracks of known dimensions were introduced into the superficial layer of healthy articular cartilage samples that were subsequently subjected these to tensile loading at known strain-rates to effect fracture propagation. It is our view that the initial cracks of 25μm to 200μm deep approximated the possible range of the sizes of cracks and fissures that could occur in the superficial zone of the matrix. We have subjected the cracks to conditions in which they experience maximum severity of loading. Previous studies have shown that high tensile stresses are generated in the knee in flexion (Minns et al. 1979), and that tensile stresses occur in the regions adjacent to the contacting, loaded surfaces in the joint (Kelly and O'Conner 1996). Therefore, despite the fact that the joint is mostly subjected to compressive loading, a tensile loading regime is the most likely condition for crack propagation.

The development in this study focuses on the understanding of the behaviours of two geometrical characteristics of the growing crack, and one property of the global matrix. Specifically, we analyse the parameters *db* and *dc* which measure the opening of the crack mouth and the length of the slanting edge as the crack stretches, respectively. The parameter *dh* represents the displacement of the bottom layer relative to its initial horizontal position. This parameter measures the response of the matrix as the crack stretches and it is due to the pull of the collagen fibres on the bottom layer in response to the tensile load (Stok and Oloyede 2003).

Following the geometry and loading of the fracture specimens adopted in this study, we were able to categorise the different fracture patterns in cartilage samples leading to the development of plausible parameters for the characterisation of the resistance of the cartilage matrix to the growth of a crack initiated wholly within its superficial zone. In this regard we have quantified the physical parameters of the nonlinear process, for example, *dh* which represents the gross necking of the sample as the matrix progresses towards final failure.

Because *dh* characterises the necking, it is our opinion that it can be used to establish a fracture parameter for the tissue. However, we note that this parameter is not directly related to the geometrical attributes of the crack. Plotting *dh* against *dc*, which is a crack edge length, shows a consistent one-to-one correspondence between the two parameters ($dc = 0.93dh$). On the other hand a repeatable non-linear relationship was found to exist between *dh*, and the crack mouth opening *db*, namely, $db = 0.58dh^2 + 0.35dh$, consequently, we have recommended using the critical crack edge length *dc* instead of *dh* or *db* in cartilage fracture analysis. It is worth noting that *dh* always grows progressively to a critical value as the bottom layer deforms progressively towards the crack root, and is matched by a measurable value of *dc*, the crack stretch.

Both parameters *dh* and *dc* reach their final values at the point of fracture, and we define the value of *dc* at this point as c_{ps}. Consequently, the critical crack dimension at which unstable fracture propagation begins is represented by c_{ps}.

A note on the use of the stretch parameter c_{ps}

In equation 3, we have used the parameter c_{ps} to characterise the crack at the point of failure. This parameter appears as a deviation from conventional fracture mechanics, however, it is simply a representation of the usual crack length of classical fracture mechanics in a manner that reflect the This is because it is apparent from our experiments that while the initial crack length did not extend under the applied load, the crack still grew with the stretch of its edge

which we have represented by the length *dc*, with the angle between this crack edge and the vertical line drawn through the crack tip increasing until the edge is practically parallel to the horizontal axis drawn through the middle of the sample. The sample fractured by the time this initially vertical edge becomes almost horizontal following a period of extension in response to the applied load. With respect to figure 1B, the following relationship can be written between the crack length *da* and the crack edge *dc*, if the angle between them is $d\phi$ and they a right angle triangle is completed by *da*, *dc* and *db*: $da = dc\,(\cos d\phi)$. Therefore, with further deduction from our video analysis we made the mathematical deduction that as $a \to a_{crit}.\ and\ \phi \to \pi;\ c \to c_{ps}$, so that the critical crack length $a_{crit} \approx c_{ps}$. With these approximations it is possible to substitute the parameter exhibiting noticeable growth namely the stretch parameter c_{ps} for the practically stagnant crack length in the fracture toughness calculation. Of importance is that these two parameters are related and that the manifestation of the fracture progression is adequately represented by a parameter which is not the conventional crack length, but one which is closely related to it.

A fundamental basis of analysis in our present work is the ability to characterise the mechanical response of articular cartilage containing surface only cracks. In this respect, figure 1 presents the different patterns of the stress-strain responses of articular cartilage containing a superficial crack under tensile load. These curves reveal that regardless of the size of the initial crack, the tissue either exhibits brittle fracture (figure 1b) or an initial brittle fracture followed by a period of stable crack growth that eventually ends with sudden fracture (fig. 1 a, c, d and e). Of importance to this work is that these responses show that it is possible to describe cartilage fracture with relationships similar to those used in linear elastic fracture mechanics. For the present analysis, we have assumed that the work done up to the point of maximum stress, after which rapid growth occurs is the work required to propagate a crack to final failure. It is however, important to note that while the strain induced did not seem to vary significantly between samples along different spilt-lines, it is important to note that the other parameters of

deformation such as failure stress, compliance and tangent modulus varied with split-line direction. It is therefore important that this spilt-line orientation-dependence should be taken into account when evaluating the fracture parameters of articular cartilage.

4.1 A Fracture Parameter for Articular Cartilage

Using the critical crack edge parameter, c_{ps} as a substitute for the critical crack length in the linear elastic fracture mechanics fracture toughness, and comparing the result to those based on ASTM standards which use a function of the geometry correction factor f(a/w) (figure 7), demonstrates that using the critical crack edge length produces a viable fracture toughness for articular cartilage. Figure 7d demonstrates that this new parameter meets the condition of invariability demanded for fracture toughness which is a material characteristic or constant. Therefore, a new parameter of analysis, $c_{ps,}$ is now suggested for correlating and analysing fracture propagation in articular cartilage when the sample contains an initiated crack which is wholly confined within the articular surface. Using the new methodology, rate-dependent poroelastic fracture toughness, Kp_{Ic} was calculated across the range of strain-rates and initial crack lengths. With regard to the loading rate, it can be seen that neither the difference in strain-rate from 0.0016 to 0.0048s^{-1}, nor the small width, B, had a discernible effect on the value of the poroelastic fracture toughness. Although the width, B was small, the ratio $^{B}/_{W}$ was in fact quite large, and maintained within the ASTM recommendations, so that despite its thinness, the fracture model seem to resemble that seen in much thicker materials where the bulk material resists both deformation and fast crack growth, consequently, it can be concluded that the tissue behaves as if the crack was under a plane strain, rather than a plane stress constraint despite its thinness. The energy dissipation associated with fluid exudation may have contributed to this apparent plane strain-type response, such that the energy available for crack propagation is continuously reduced as fluid is squeezed out of the matrix under load.

5. Conclusion

This work has shown that an appropriate modification of classical fracture mechanics can be used to define the crack resistance of articular cartilage. The poroelastic fracture toughness of articular cartilage, where cracks are initiated within the articular surface and allowed to propagate through the general matrix to failure under tension, is Kp_{Ic} = 1.83 (SD = 0.8) MPa.$\sqrt{\text{mm}}$. It has been demonstrated that the unorthodox crack growth mechanism seen in articular cartilage can be measured and quantified as a poroelastic fracture parameter, and further work should focus on applying this knowledge to consider the change in fracture toughness with degrading tissue structure and exploring the possibilities for a clinically useful failure criterion.

FIGURE 1

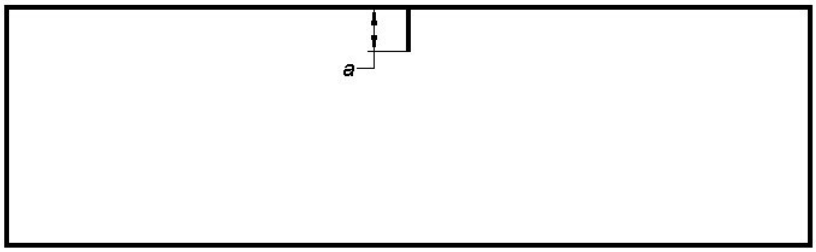

(A)

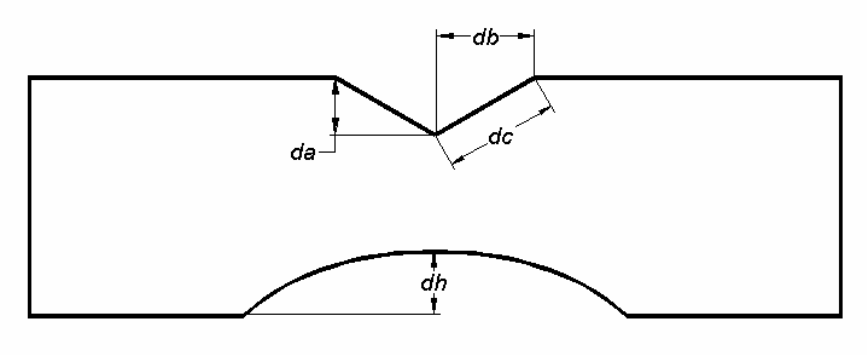

(B)

FIGURE 2

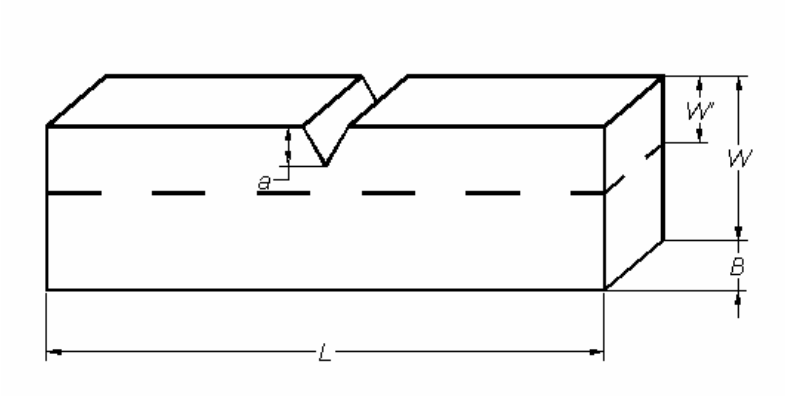

FIGURE 3

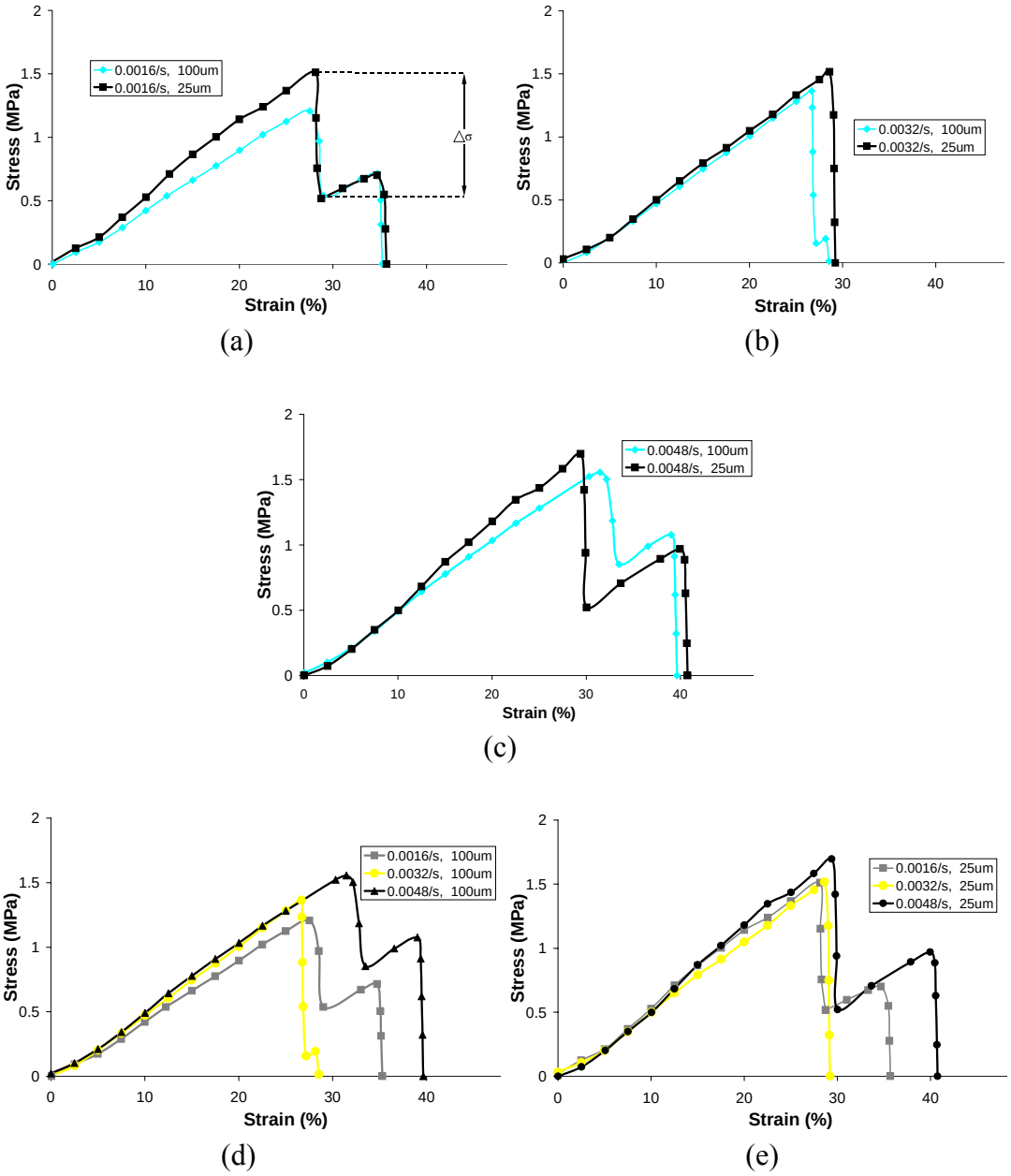
Stress (MPa)
Strain (%)
0.0016/s, 100um
0.0016/s, 25um
△σ
(a)
0.0032/s, 100um
0.0032/s, 25um
(b)
0.0048/s, 100um
0.0048/s, 25um
(c)
0.0016/s, 100um
0.0032/s, 100um
0.0048/s, 100um
(d)
0.0016/s, 25um
0.0032/s, 25um
0.0048/s, 25um
(e)

FIGURE 4

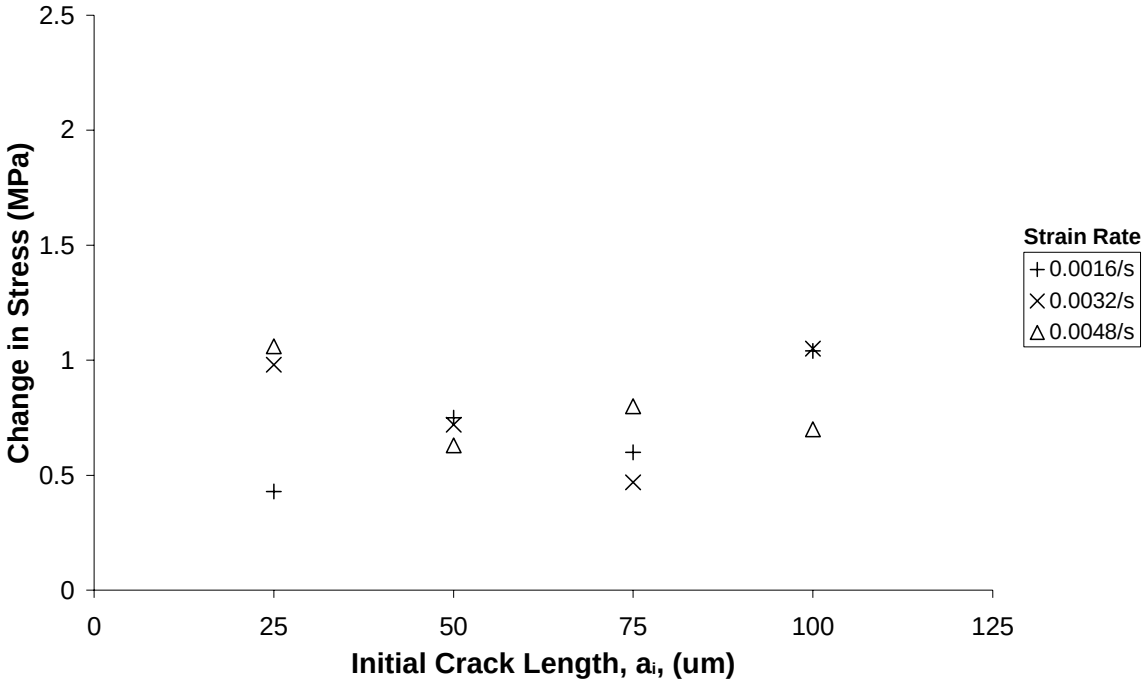

FIGURE 5

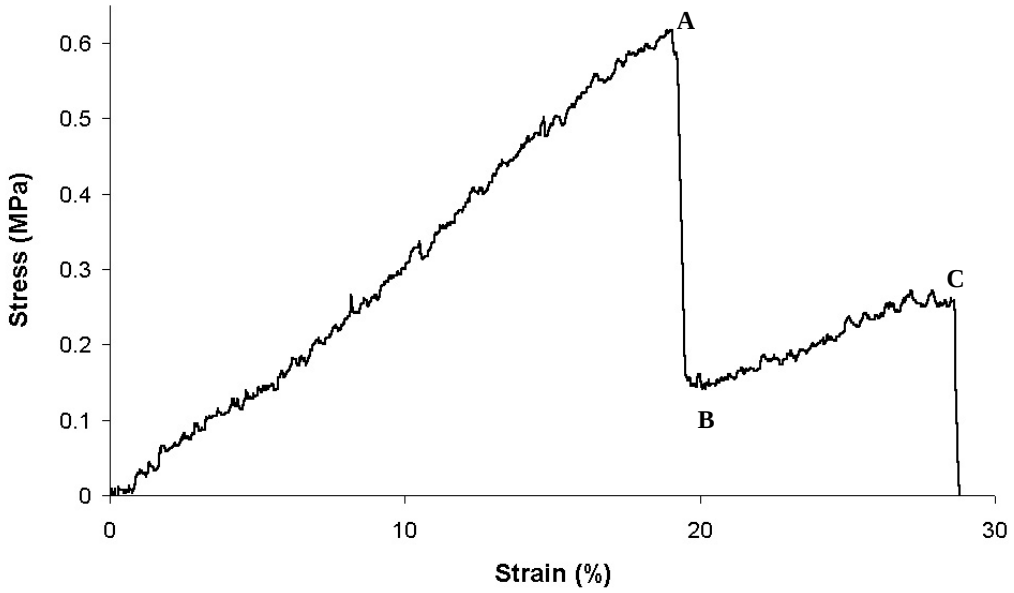

FIGURE 6

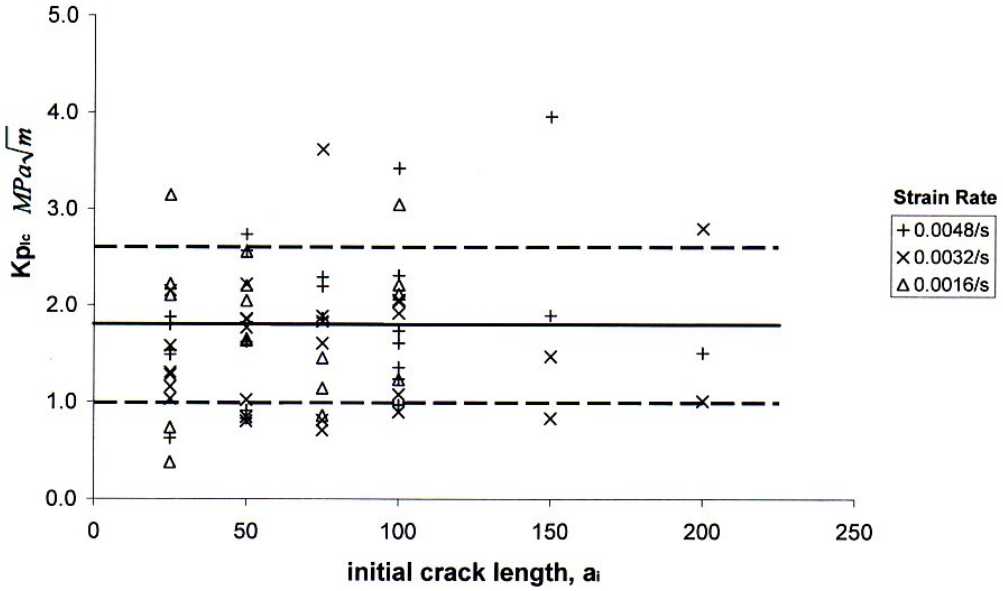

FIGURE 7

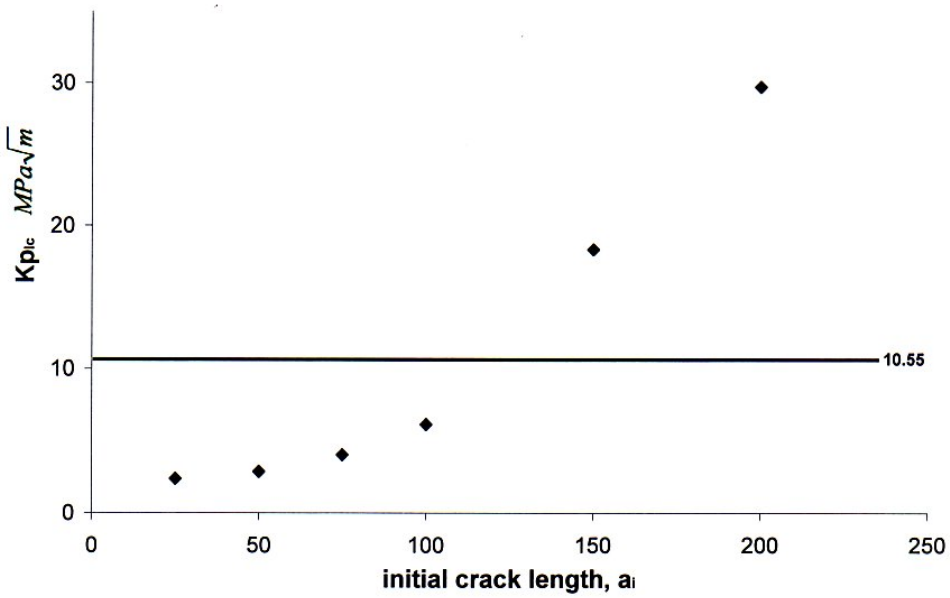

(a)

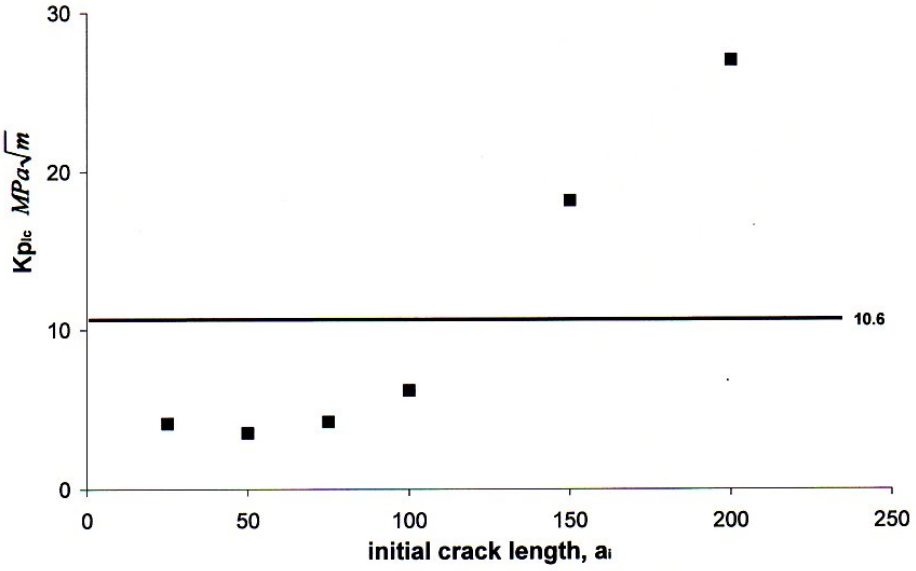
30
20
10
0
Kpic MPa√m
10.6
0
50
100
150
200
250
initial crack length, ai

(b)

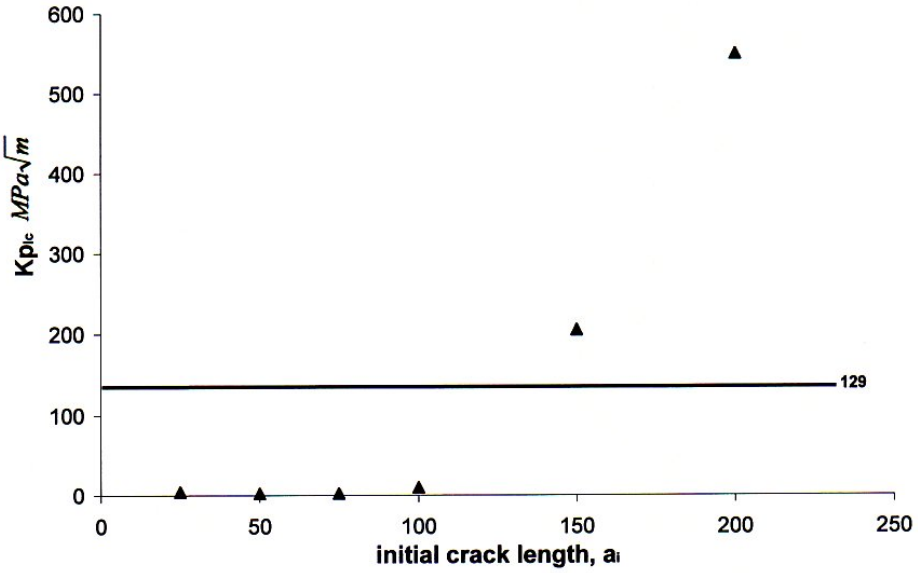
600
500
400
300
200
100
0
Kpic MPa√m
129
0
50
100
150
200
250
initial crack length, ai

(c)

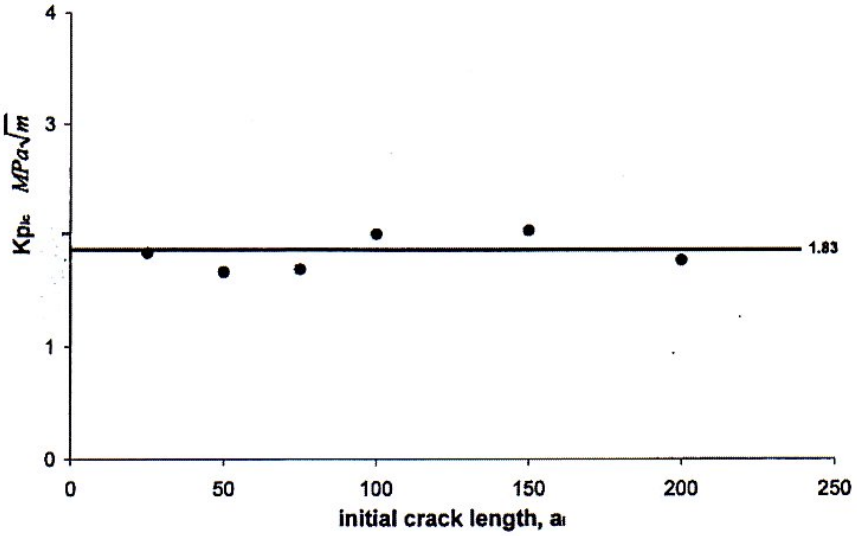

(d)

Table 1: Mean values of measured mechanical properties for the medial and lateral patella surfaces, (n = number of specimens).

		Medial		Lateral	
		n	*mean (SD)*	*n*	*mean (SD)*
Maximum Load (N)		100	4.42 (2.20)	73	4.99 (2.50)
Maximum Stress (MPa)		101	1.87 (1.05)	73	1.61 (0.87)
Strain Energy per unit volume (MPa)		101	0.39 (0.38)	73	0.36 (0.35)
Tangent Modulus (MPa)	- 2.5%	101	4.17 (1.75)	73	3.50 (1.45)
	- 20%	75	6.69 (2.74)	56	5.07 (1.97)
Compliance (MPa^{-1})	- 2.5%	101	1.74 (0.91)	73	1.69 (0.91)
	- 20%	75	1.09 (0.34)	56	1.09 (0.43)

Table 2: Compliance measurements (MPa^{-1}) at different loading rates for the medial and lateral patella surfaces, mean (SD), P= p-value.

Strain-rate (s^{-1}) →		0.0016	0.0032	0.0048	P
			Medial		
Strain →	2.5%	1.77 (1.04)	1.64 (0.68)	1.82 (1.01)	0.726
	20%	1.10 (0.39)	1.17 (0.36)	1.04 (0.27)	0.405
			Lateral		
	2.5%	1.71 (1.08)	1.64 (0.58)	1.70 (0.92)	0.969
	20%	1.18 (0.65)	1.06 (0.19)	1.03 (0.25)	0.494

Table 3: Compliance measurements (MPa^{-1}) at different initial crack lengths for the medial and lateral patella surfaces, mean (SD), P = p-value.

Crack length (μm)→		0	25	50	75	100	P
				Medial			
Strain →	2.5%	1.46 (0.70)	1.76 (0.71)	1.45 (0.46)	1.96 (1.32)	2.07 (1.04)	0.097
	20%	1.07 (0.33)	1.06 (0.44)	1.04 (0.24)	1.17 (0.42)	1.10 (0.27)	0.867
				Lateral			
	2.5%	1.39 (1.22)	1.69 (1.09)	1.87 (0.98)	1.71 (0.74)	1.62 (0.58)	0.809
	20%	0.77 (0.17)	0.98 (0.24)	1.08 (0.30)	1.21 (0.38)	1.38 (0.70)	0.024

Table 4: Mean values of measured mechanical properties for specimens tested along and across the split-line direction, (n = number of specimens).

		Across (m-l)		Along (a-b)	
		n	*mean (SD)*	*n*	*mean (SD)*
Failure Stress (MPa)		131	1.58 (0.93)	43	2.31 (0.97)
Tangent Modulus (MPa)	- 2.5%	131	4.03 (1.62)	43	3.45 (1.71)
	- 20%	93	5.53 (2.44)	39	7.14 (2.52)
Compliance (MPa^{-1})	- 2.5%	131	1.78 (0.71)	43	2.30 (1.18)
	- 20%	93	1.26 (0.42)	39	1.08 (0.26)

Table 5: Compliance measurements (MPa^{-1}) at different loading rates for specimens tested along and across the split-line direction, mean (SD), P = p-value.

Strain-rate (s^{-1}) →		0.0016	0.0032	0.0048	P
			Across (m-l)		
Strain →	2.5%	1.56 (0.91)	1.57 (0.58)	1.43 (0.52)	0.633
	20%	1.26 (0.57)	1.25 (0.33)	1.19 (0.25)	0.176
			Along (a-b)		
	2.5%	2.35 (1.27)	2.03 (0.88)	2.37 (1.27)	0.790
	20%	1.05 (0.30)	1.04 (0.22)	1.08 (0.26)	0.727

Table 6: Compliance measurements (MPa^{-1}) at different initial crack lengths for specimens tested along and across the split-line direction, mean (SD), P = p-value.

Crack length (μm)→		0	25	50	75	100	P
				Across (m-l)			
Strain →	2.5%	1.43 (0.89)	1.62 (0.87)	1.53 (0.52)	1.61 (0.73)	1.47 (0.46)	0.855
	20%	1.00 (0.35)	1.05 (0.35)	1.09 (0.28)	1.26 (0.50)	1.23 (0.65)	0.338
				Along (a-b)			
	2.5%	1.48 (0.64)	2.27 (0.99)	3.13 (1.70)	2.17 (1.38)	2.57 (1.03)	0.326
	20%	0.98 (0.18)	0.87 (0.24)	0.89 (0.06)	1.13 (0.29)	1.20 (0.25)	0.069

Table 7: Tangent moduli (MPa) of undamaged specimens at two strain levels for all strain-rates, mean (SD).

Strain-rate (s^{-1})	**0.0016**	**0.0032**	**0.0048**
Strain			
2.5%	4.74 (2.13)	4.42 (1.95)	4.46 (1.65)
20%	6.19 (2.69)	6.60 (2.27)	6.25 (1.86)

Table 8: Gp_{Ic} at the 2.5% and 20% strain levels.

	Gp_{Ic} (kN/m)	
Strain (%)	*mean, μ*	*standard deviation, SD*
2.5	0.736	0.536
20	0.532	0.385

Figure Captions

Figure 1: Schematic of the crack growth dimensions in articular cartilage (b) containing an initial crack, *a* (a).

Figure 2: Schematic illustrating specimen dimensions (not to scale), where B = width, W = overall thickness, W' = thickness of the superficial zone, L = specimen length, and a = crack length.

Figure 3: Plots of typical stress-strain curves comparing rate of loading and initial crack length. (a-c). Specimens with 25μm initial crack lengths show a higher maximum stress. (d, e) Tangent moduli are similar for the three loading rates for either 25 or 100μm. Figure (a) includes Δσ, i.e. phase of rapid crack growth.

Figure 4: Typical curve showing the change in stress (Δσ) against initial crack length, for the three rates of loading.

Figure 5: Typical stress-strain curve identifying points of central interest. AB: period of rapid crack propagation, BC: short period of stable crack growth, and C: catastrophic failure.

Figure 6: Mean value of Kp_{Ic} for pooled data. (Dashed lines represent one standard deviation from the mean, bold line.)

Figure 7: Determination of Kp_{Ic} using (a) ASTM(1) solution for $f(a/W)$, (b) using ASTM(2) solution for $f(a/W)$, (c) using Chin-Purcell and Lewis' solution for $f(a/W)$, and (d) using current analysis of critical stress and crack growth, c_{ps}, where it can be seen that variation with a is minimal. ♦ represents the average value of all specimens for a given crack length, — indicates the average Kp_{Ic} for the data, assuming strain rate and initial crack length do not affect Kp_{Ic}.

References

Akizuki, S., Mow, V.C., Muller, F., Pita, J.C., Howell, D.S., and Manicourt, D.H., 1986. Tensile properties of human knee joint cartilage: I. influence of ionic conditions, weight bearing, and fibrillation on the tensile modulus. J. of Orthop Res., 4, 379-392.

ASTM, 1990. Standard test methods for plane-strain fracture toughness of metallic materials. American Society for Testing and Materials.

Broom, N.D., 1984. Further insights into the structural principles governing the function of articular cartilage. J. Anat. 139, 275-294.

Broom, N.D. and Marra, D.L., 1985. New structural concepts of articular cartilage demonstrated with a physical model. Connective Tissue Res., 14, 1-8.

Chin-Purcell, M.V. and Lewis, J.L., 1996. Fracture of articular cartilage. J. Biomech Engrg 118, 545-556.

. Clarke, I.C., 1971. Articular cartilage: a review and scanning electron microscope study I. the interterritorial architecture. J. Bone Joint Surg. 53B, 732-750.

Ewalds, H.L. and Wanhill, R.J.H., Fracture Mechanics. 1991, Edward Arnold, Melbourne.

Finlay, J.B. and Repo, R.U., 1978. Instrumentation and procedure for the controlled impact of articular cartilage. IEEE Trans Biomed Eng, 25, 34-39.

Frost, H.M., 1999. Joint anatomy, design, and arthroses: insights of the Utah paradigm. The Anatomical Record, 255, 162-174.

Glenister, T.W., 1976. An embryological view of cartilage. J. Anat., 122, 323-330.

Kempson, G.E., Spivey, C.J., Swanson, S.A.V., and Freeman, M.A.R., 1971. Patterns of cartilage stiffness on normal and degenerate human femoral heads. J. Biomech, 4, 597.

Lipshitz, H., Etheredge III, R., and Glimcher, M.J., 1976. Changes in the hexosamine content and swelling ratio of articular cartilage as functions of depth from the surface. J Bone Joint Surg, 58A, 1149-1153.

McCormack, T. and Mansour, J.M., 1998. Reduction in tensile strength of cartilage precedes surface damage under repeated compressive loading *in vitro*. J. Biomech, 31, 55-61

Meachim, G., 1980. Cartilage breakdown, In: Scientific Foundations of Orthopaedics and Traumatology, 290-296.

Meachim, G., 1972. Light microscopy of indian ink preparations of fibrillated cartilage. Annals Rheu Dis, 31, 457-464.

Meachim, G. and Roy, S., 1969. Surface ultrastructure of mature adult human articular cartilage. J Bone Joint Surg, 51B, 529-539.

Minns, R.J., Birnie, A.J.M., and Abernathy, P.J., 1979. A stress analysis of the patella, and how it relates to patellar articular cartilage lesions. J. Biomech, 12, 699-711.

Morrison, J.B., 1970. The mechanics of the knee joint in relation to normal walking. J. Biomech, 3, 51-61.

Morrison, J.B., 1968. Bioengineering analysis of force actions transmitted by the knee joint. Biomed Engng, 3, 164-170.

Oloyede, A., Flachsman, R., and Broom, N.D., 1992. The dramatic influence of loading velocity on the compressive response of articular cartilage. Connective Tissue Res 27, 1-15.

Purslow, P.P., 1983. Measurement of the fracture toughness of extensible connective tissues. J. Mat Sci., 18, 3591-3598.

Radin, E.L., Parker, H.G., Pugh, J.W., Steinberg, R.S., Paul, I.L., and Rose, R.M., 1973. Response of joints to impact loading - III. relationship between trabecular microfractures and cartilage degeneration. J. Biomech., 6, 51-57.

Radin, E.L., Paul, I.L., and Lowy, M., 1970. A comparison of the dynamic force transmitting properties of subchondral bone and articular cartilage. J Bone Joint Surg, 52A, 444-456.

Rivlin, R.S. and Thomas, A.G., 1953. Rupture of rubber. I. characteristic energy for tearing. J. Polymer Sci., 10, 291-318.

Stok, K. and Oloyede, A., 2003. A qualitative analysis of crack propagation in articular cartilage at varying rates of tensile loading. Connective Tissue Res., 44, 2, 109-120.